ANALYSIS OF MAGNETOHYDRODYNAMIC CONVECTIVE HEAT TRANSFER OF CASSON NANOFLUID FLOW OVER A HEATED STRETCHING VERTICAL PLATE

JOHN KINYANJUI KIGIO (BSc. Mathematical Sciences, with IT)

I56/39148/2016

A research project submitted in partial fulfilment of the requirements for the award of the Degree of Master of Science (Applied Mathematics) in the School of Pure and Applied Sciences of Kenyatta University

APRIL, 2022

DECLARATION

Declaration by the Candidate

This project is my original work and has not been submitted for any award of a degree in any University.

Name: John Kinyanjui Kigio

Signature: .....

Date: .....

Declaration by the Supervisor

This project has been submitted for examination with my approval as the University Supervisor

Name: Dr. Winifred Nduku Mutuku

Signature: .....

Date: .....

Department of Mathematics and Actuarial Science

Kenyatta University.

Dedication

I dedicate this work to my late mother, Ruth Kigio Wanyoike

Acknowledgement

First of all, I thank the Almighty God for giving me the strength to do this project. Secondly, I am very thankful to my supervisor, Dr. Winifred Mutuku for her insights and contribution to the success of this work. Indeed, she never lost hope in me despite the constant reminders of the need to get this done. I would also wish to thank member of staff in the Department of Mathematics & Actuarial Science, Kenyatta University who assisted me in one way or another in this journey. Thirdly, I appreciate Samuel Abayomi Oke who kept me on toes as I did this project. Indeed, you changed my perspective on Fluid Mechanics!. Lastly, I wish to thank Weldon,Halson, Kinoti, Derrick, Kioko, Belindar, Victor, Komu, just to mention a few for the concern they had as I did the work.

Abstract

Casson fluid has many industrial and engineering applications. However, Casson nanofluid possesses superior electrical and thermal conductivities compared with the original Casson fluid. Hence, the Casson nanofluid is considered in this project. The equation governing the natural convective magnetohydrodynamics flow of Casson nanofluid across a a convectively heated vertical plate is formulated. The equation is reformulated into a system of ordinary differential equations (ODEs) using similarity transformations. Thereafter, a numerical solution of the resulting ODEs is obtained using the Runge-Kutta-Gills method. It is found that flow temperature profiles increase with increasing Eckert number, Biot number and magnetic field strength while flow velocity decreases as the flow becomes Newtonian and as nanoparticle volume fraction increases.

Abbreviations and Symbols

Symbols					
T	Temperature	u, v	velocity components in the x, y- directions		
c_p	Specific heat capacity	C	Concentration of nanoparticle		
n	Velocity index	g	Acceleration due to gravity		
B_0	magnetic field strength	μ	Coefficient of dynamic viscosity		
σ	electrical conductivity	β_T, β_C	coefficient of thermal and concentration expansion		
γ	Casson fluid parameter	D_B, D_T	Brownian and thermophoretic diffusion coefficient		
κ	thermal conductivity	T_w, T_∞	Wall and free stream temperature		
α	thermal diffusivity	C_w, C_∞	Wall and free stream concentration		
ρ	fluid density	ϕ	nanoparticle volume fraction		
Subscripts					
nf	Nanofluid	bf	base fluid	np	nanoparticle

Table of Contents

List of Figures

Chapter 1
Introduction

1.1 Background Information

Fluid is any substance that flows or deforms under applied shear stress regardless of the magnitude of the applied stress. It consists of a subset of the states of matter and include liquids, gases and plasma. Fluids differ from solid by its reaction to stress. A solid exhibit a small deformation that does not change with respect to time. It implies that liquids cannot return to their original form after deformation. Fluids can be classified into two major categories, that is, Newtonian and Non-Newtonian fluids. Newton's law of viscosity defines the relationship between the shear stress and rate of a fluid (that is, shear thinning and thickening) when subjected to mechanical stress. Newtonian fluids (such as water, air, alcohol, glycerol, and thin motor oil) are those that obey the law while non-Newtonian fluids do not follow the law. Examples of non-Newtonian fluids are custard, starch suspension, corn starch, paint, melted butter, and shampoo. In non-Newtonian fluids, shear stress and rates are not linearly related. In real industrial applications, non- Newtonian fluids are more appropriate than Newtonian fluids. Non-Newtonian fluids have wide industrial applications such as drag reduction, transpiration cooling, design of thrust bearings etc. A fluid is said to be shear thickening if its viscosity increases as the shear rate increases. Shear thinning is a property of non-Newtonian fluids where the viscosity decreases under shear strain. Casson fluid model is as a shear thinning non-Newtonian fluid model possessing yield stress below which no flow occurs. It has been found that the Casson fluid accurately models fluids such as honey, toothpaste, blood etc. Nanofluids are suspensions of nanoparticles in fluids, causing a significant enhancement of their properties at limited nanoparticle concentrations. The nanoparticles used in

nanofluids are typically made of metals, oxides, carbides, or carbon nanotubes. They are widely used for as coolants in heat transfer equipment such as radiators, heat exchangers and electronic cooling system. Nanofluids have enhanced thermal conductivity property and the convective heat transfer coefficient compared to the base fluid.

Hannes Alfven (1908-1995) introduced the branch of physics that studies the properties of electromagnetism, which in turn birthed the area of fluid dynamics called magnetohydrodynamics (MHD). MHD is the study of magnetic properties in electrically conducting fluids, such as plasmas, liquid metals, salt water, and electrolytes. The result of the interaction between an electrically conducting fluid and a magnetic field is the electromagnetic behaviours exhibited in the flow. To unravel MHD flow properties, the basic equations of fluid flow (continuity, momentum and energy equations) coupled with Maxwell's equations of electromagnetism. These MHD equations play a critical role in a variety of areas in engineering, space-physics and astrophysics.

Heat transfer describes the flow of thermal energy (i.e., heat) due to differences in temperature distribution. The second law of thermodynamics establishes that heat flows from a region of higher temperature to a region of lower temperature, unless the process is artificially conditioned. Heat transfer occurs only in three modes; conduction, convection, and radiation. The convective heat transfer is the transfer of heat between two surfaces without physical contact and it is common in liquids and gasses. Convection occurs when the temperature of the surface differs from that of the surrounding fluid. Convective heat transfer can be forced or free convection. In free convection, the fluid motion is caused by natural means such as the buoyancy effects while in forced convection the motion is forced by external means such as a pump.

In this project, flow properties of a natural convective heat transfer in a magnetohydrodynamics flow of Casson base-fluid in which copper nanoparticles are suspended shall be analysed.

1.2 Statement of the Problem

Convective heat transfer is one of the most natural phenomena observed in fluid flow and this has attracted attention over the years. Several studies have been carried out to unravel the effect of natural convection on flow properties and some have even extended the research to forced convection. It was also realised that extent of the influence of convective heat transfer in a flow depends largely on the nature of fluid under consideration. This study considers the Casson nanofluid because of its extensive applications in many engineering and technology industries. Despite the rapt attention of researchers to the superiority of the thermophysical properties of the nanofluid over the base fluid and the macrosized particles, none has studied the simultaneous effect of convective heat transfer and convectively heated boundary on a magnetohydrodynamic flow of Casson nanofluid. This project is motivated to address this research gap. A natural convective heat transfer in magnetohydrodynamic flow of Casson nanofluid over a convectively heated stretching vertical surface shall be analysed in this project.

1.3 Objectives

1.3.1 General Objective

To numerically analyse MHD convective heat transfer of a Casson nanofluid flow over a heated stretching vertical plate.

1.3.2 Specific Objectives

The specific objectives of this study are to;

i. To investigate the effects of Lorenz force on MHD Casson nanofluid flow over a heated plate

ii. To determine the effects of viscous dissipation on MHD Casson nanofluid flow over a heated plate

iii. To explore the effect of nanoparticle volume fraction on MHD Casson nanofluid flow over a heated plate

1.4 Significance of the Study

The enhanced physical and thermal properties of the nanofluid makes it very applicable in cooling processes, refrigerators, laptops etc. Most of the recent researches in fluid mechanics are on nanofluid flows. By taking the Casson fluid as the base fluid, the Casson nanofluid is invented. The Casson nanofluid is of far-reaching impact in emulsion companies, bioreactors, medical engineering etc. A more robust fluid flow is invented when powerful effect of convective boundary heating is combined with the natural convective heat transfer in the flow of Casson nanofluid under the influence of magnetic field. The results of this research shall provide more useful hints specifically to industries involved in thermocooling, vehicular fluid, magnetic drug targeting, geothermal reservoirs, heat exchangers, ablation, medical sciences, metallurgy etc.

1.5 Justification of the Study

Natural convective flow is common area of study for many researchers and a lot of progress have been made over the years. More so, since the invention of magnetohydrodynamics flow, attention

has been drawn to convective MHD flow. In fact, many researches were conducted recently on natural convective MHD Casson nanofluid flow. To the best of my knowledge, despite the extent of research on convective flows, no one has considered a convective MHD Casson nanofluid flow over a convectively heated surface. This study is therefore conducted to fill the research gap.

Chapter 2
Literature Review

A simple technique was presented by Dincer and Dost (1996) to analyse heat transfer in Absorption Cooling Systems (ACSs). Despite the simplicity of the technique, the results proved useful to generally analyse and design Absorption Cooling Systems. Yang *et al*. (1996) studied convective heat transfer across a cylinder and found that the more the distance between the cylinder and the wall, the higher the heat transfer rate and drag force. Cheng *et al*. (1998) studied heat transfer in melting processes in an elliptical tube and a semi-analytical solution was obtained. The solution revealed that melting rate increases with time. Kumar *et al.* (1998) used the finite element method (FEM) to solve the Darcian flow with convection in an isothermal sinusoidal surface. This study ensured that the limitation of the finite element method was taken care of by avoiding restrictions on the geometrical non-linearity arising from the parameters. The study revealed that increasing Raleigh number causes a transformation from unicellular to multicellular flow and more so, there is an insignificant increase in the heat transfer rate when flow geometry moves from slender to blunt. Zerroukat *et al.* (1998) adopted the collocation method with some radial basis functions to study heat transfer in different geometries while Piechowski (1998) used experimental results to validate ground heat exchanger model and carried out sensitivity analysis. Saatdjian *et al.* (1999) solved the 2D Darcy- Boussinesq equations using finite difference code over fine grid and it was found out that the heat transfer rate from the slender geometry is greater than that obtained in the blunt case in all cases. Kolenko et al. (1999) analysed total radiative heat transfer in a furnace chamber.

Mutuku-Njane and Makinde (2013) investigated an MHD nanofluid flow over a convectively heated vertical porous plate. The results indicated that increase in the magnetic field strength and nanoparticle volume fraction has retarding effects on velocity profiles but enhance temperature profiles. Ahmad *et al.* (2014) modified the work of Mutuku-Njane and Makinde (2013) to consider MHD flow towards an exponentially stretching sheet in a porous medium and in the presence of radiation effects and Darcy's resistance. The study obtained an analytical solution using the Homotopy Analysis Method (HAM) and showed that thermal boundary layer thickness decreases with increasing Prandtl number. Ahmad *et al.* (2018) studied MHD flow with the presence of internal heat source and a numerical investigation indicated that the heat transfer can be reinforced by increasing Prandtl number. In fact, it was observed that increasing thermal slip retards the flow temperature. Farooq *et al*. (2019) decided to consider nanofluid whose base fluid is the electrically conducting Maxwell fluid. Investigation of the MHD flow showed that the Lorenz force induced by magnetic field enhances the temperature and concentration of the flow. Recently, MHD flow of nanofluid was carried out with Cattaneo-Christov heat flux model (Venkateswarlu *et al*. 2020), over corrugated vibrating bottom surface (Jabeen *et al*. 2020) while some semi-analytical approaches to solving the equations were presented in Bulinda *et al*. (2020). Each of these studies observe that temperature is enhanced with increasing magnetic force.

Nadeem *et al*. (2013) investigated the Casson fluid flow past a porous linearly stretching sheet and observed that flow resistance increases with an increasing Casson parameter and magnetic field strength. The skin-friction coefficient in the x- direction increased with an increase in the stretching ratio. The coefficient of skin friction increases with increasing magnetic field strength. Meanwhile, Pramanik (2014) analysed heat transfer in Casson fluid flow on an exponentially

porous stretching surface and observed that increasing Casson fluid parameter suppresses the velocity but enhances temperature. The outcome corroborates the earlier results of Mutuku-Njane and Makinde (2013) and Nadeem *et al*. (2013). The effects of variable thermal conductivity on Casson fluid flow were also examined by Idowu et al. (2020) by studying the effects of a non-Darcian porous medium, nonlinear radiation as well as temperature dependent thermal conductivity and viscosity on Casson flow. Mahantesh *et al*. (2020) modified the work of Idowu *et al*. (2020) to include the presence of non-linear thermal radiation while the flow is over a moving vertical plate.

Mustafa and Khan (2015) modified the problem of Pramanik (2014) by extending the flow to Casson nanofluid under the influence of magnetic field and the result was still in full agreement with earlier results. The fact that the effectiveness of automotive radiators is directly related to the type of fluid used in their preparation motivated Mutuku (2016) to consider Ethylene-Glycol-based nanofluid. The results also agree with the existing results. A further extension was conducted by Kataria and Patel (2018) to consider an oscillating vertical plate. An analytic solution was obtained using the Laplace Transform and expressions were obtained for the dimensionless velocity and temperature. The work of Idowu *et al*. (2020) was extended by Gbadeyan *et al*. (2020) to Casson nanofluid to examine the effects of a non-Darcian porous medium, nonlinear radiation as well as temperature dependent thermal conductivity and viscosity on Casson nanofluid flow. Shah *et al*. (2020) also extended the work of Mahantesh *et al.* (2020) to Casson nanofluid. All these researches came out with the same outcomes that Casson fluid parameter causes a reduction in the velocity but an increase in the temperature. From the aforementioned literature, it is clear that no one has

considered convective magnetohydrodynamics flow of Casson nanofluid over a convectively heated surface. This project is motivated to fill this research gap.

Chapter 3
Governing Equations

Figure (1) shows the flow of Casson nanofluid over a vertical plate under the action of a magnetic field. The Casson nanofluid is made up of Casson base-fluid and copper nanoparticles. The x-axis is taken as the vertical axis and the y-axis as the horizontal axis, so that the direction of flow is on the x-direction. The flow is in a direction opposite gravity so that the acceleration due to gravity is taken as g. A magnetic field is applied parallel to the y-axis and the strength of the magnetic field is taken as a constant B_0. The presence of the magnetic field induces the Lorentz force which opposes the flow. The wall surface is subjected to convective heating boundary condition. The convective heating condition is such that the rate of change of the temperature at the wall is the difference of the instantaneous temperature and the free stream temperature and it is mathematically given as;

$$-k_f \frac{\partial T}{\partial y} = h_f(T - T_\infty),$$

where k_f is convective thermal conductivity and T_∞ is the free stream temperature. The no-slip condition is assumed in the flow. Hence, for a linearly stretching vertical surface, the wall velocity in the x-direction is $U_w = ax$ where ax is the linear stretching applied to the surface. The wall velocity in the y-direction is 0 since the wall is not moving in the y-direction. Also, the wall temperature obeys the convective surface heating. The free stream conditions are also given so that the temperature and the velocity at the free stream are 0 and T_∞ respectively. Figure (1) below gives a description of the flow; showing the direction of flow, the nanoparticles, the magnetic field and the surface.

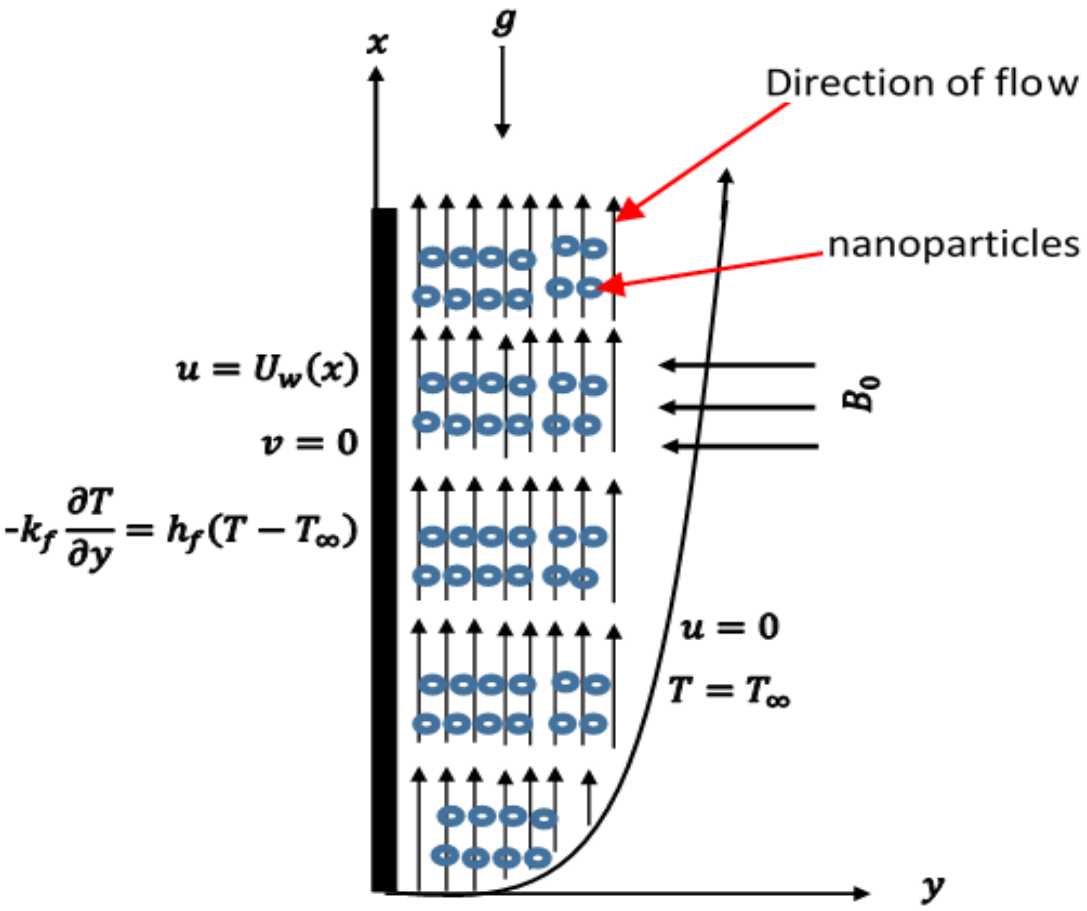

Figure 1: *Flow schematic diagram*

We formulate the equations governing the natural convective flow of electrically conducting Casson nanofluid under the influence of magnetic field by introducing the Casson constitutive equations in the Navier-Stokes equation and including the magnetic and buoyancy body forces. After performing the boundary layer analysis to ensure consistency in the order of magnitude, the continuity equation, momentum equation, energy equation and the species equation are obtained.

The continuity equation of the two-dimensional flow is

$$\frac{\partial u(x,y)}{\partial x}+\frac{\partial v(x,y)}{\partial y}=0, \tag{3.1}$$

The momentum equation is

$$u\frac{\partial u}{\partial x}+v\frac{\partial u}{\partial y}=\frac{\mu_{nf}}{\rho_{nf}}\left(1+\frac{1}{\gamma}\right)\frac{\partial^2 u}{\partial y^2}+g\beta_T(T-T_\infty)+g\beta_C(C-C_\infty)-\frac{\sigma_{nf}B_0^2u}{\rho_{nf}}, \tag{3.2}$$

The energy equation is

$$u\frac{\partial T}{\partial x}+v\frac{\partial T}{\partial y}=\alpha_{nf}\frac{\partial^2 T}{\partial y^2}+\tau\left(D_B\frac{\partial C}{\partial y}\frac{\partial T}{\partial y}+\frac{D_T}{T_\infty}\left(\frac{\partial T}{\partial y}\right)^2\right)+\frac{\mu_{nf}}{(\rho c_p)_{nf}}\left(\frac{\partial u}{\partial y}\right)^2+\frac{\sigma_{nf}B_0^2u^2}{(\rho c_p)_{nf}}, \tag{3.3}$$

The concentration equation is

$$u\frac{\partial C}{\partial x}+v\frac{\partial C}{\partial y}=D_B\frac{\partial^2 C}{\partial y^2}+\frac{D_T}{T_\infty}\frac{\partial^2 T}{\partial y^2}. \tag{3.4}$$

subject to the boundary conditions

$$\text{at}\quad y=0:\ u=U_w(x)=ax,\ \ v=0,\quad -k_f\frac{\partial T}{\partial y}=h_f\left(T_f-T\right),\ \ C=C_w(x), \tag{3.5}$$

$$\text{as}\quad y\to\infty:\ u\to 0,\quad T\to T_\infty,\quad C\to C_\infty, \tag{3.6}$$

where

$$\alpha_{nf}=\frac{\kappa_{nf}}{(\rho c_P)_{nf}},$$

$$\tau=\frac{(\rho c_p)_{np}}{(\rho c_p)_{bf}}.$$

Using the models proposed by Wasp (1977), Pak and Cho (1998), Xuan and Roetzel (2000), Maiga et al. (2004), the thermal conductivity is

$$\frac{k_{nf}}{k_{bf}} = \frac{k_{np} + 2k_{np} - 2\phi\left(k_{bf} - k_{np}\right)}{k_{np} + 2k_{bf} + \phi\left(k_{bf} - k_{np}\right)}, \tag{3.7}$$

the effective density is

$$\rho_{nf} = (1 - \phi)\rho_{bf} + \phi\rho_{np}, \tag{3.8}$$

the specific heat capacity is

$$\left(\rho c_p\right)_{nf} = (1 - \phi)\left(\rho c_p\right)_{bf} + \phi\left(\rho c_p\right)_{np} \tag{3.9}$$

and the viscosity is

$$\mu_{nf} = (1 + 7.3\phi + 123\phi^2)\mu_{bf}. \tag{3.10}$$

Chapter 4
Methodology

The approach for solving the system of nonlinear partial differential equations governing the fluid flow involves three steps. The first step is to nondimensionalise the partial differential equations to obtain a system of ordinary differential equations. The second step is to set the ordinary differential equations into the standard form that can be solved using MATLAB bvp4c; which uses the Runge-Kutta-Gills method. The final step is to simulate the solution and depict the simulations in graphs.

4.1 Nondimensionalisation of the governing equations

The governing partial differential equations (3.1 – 3.4) shall be converted to nonlinear ordinary differential equations using the similarity variables

$$\eta = y\sqrt{\left(\frac{a}{\nu}\right)},\ u = \frac{\partial \psi}{\partial x},\ v = -\frac{\partial \psi}{\partial y}, \tag{4.1}$$

$$T = T_\infty + (T_w - T_\infty)\theta,\ C = C_\infty + (C_w - C_\infty)\phi \tag{4.2}$$

from which the stream function is obtained as

$$\psi = \sqrt{a\nu}xf(\eta). \tag{4.3}$$

Consequently choosing u and v to satisfy the continuity equation as

$$u = axf',\ v = -\sqrt{a\nu}f(\eta). \tag{4.4}$$

From the ongoing, we have

$$\frac{d\eta}{dy}=\sqrt{\left(\frac{a}{\nu}\right)};\ \frac{\partial u}{\partial x}=af';\quad \frac{\partial u}{\partial y}=0;\quad \frac{\partial^2 u}{\partial y^2}=\frac{d\eta}{dy}\frac{d}{d\eta}\left(\frac{\partial u}{\partial y}\right)=\left(\frac{a^2x}{\nu}\right)f'''(\eta);$$

$$T=T_\infty+(T_w-T_\infty)\theta;\ \frac{\partial T}{\partial x}=0;\ \frac{\partial T}{\partial y}=\left(\frac{a}{\nu}\right)^{\frac{1}{2}}(T_w-T_\infty)\theta';\ \frac{\partial^2 T}{\partial y^2}=\left(\frac{a}{\nu}\right)(T_w-T_\infty)\theta'';$$

$$C=C_\infty+(C_w-C_\infty)\Phi;\ \frac{\partial C}{\partial x}=0;\ \frac{\partial C}{\partial y}=\left(\frac{a}{\nu}\right)^{\frac{1}{2}}(C_w-C_\infty)\Phi';\ \frac{\partial^2 C}{\partial y^2}=\left(\frac{a}{\nu}\right)(C_w-C_\infty)\Phi''.$$

The continuity equation (3.1) is satisfied by the choice of u and v in (3.12). Hence, we proceed by making the momentum equation dimensionless as follows;

$$u\frac{\partial u}{\partial x}+v\frac{\partial u}{\partial y}=\big(axf'(\eta)\big)\big(af'(\eta)\big)-\left((av)^{\frac{1}{2}}f(\eta)\right)\left(\left(\frac{a}{\nu}\right)^{\frac{1}{2}}axf''^{(\eta)}\right)=a^2x(f'f'-ff'')$$

and

$$\frac{\mu_{nf}}{\rho_{nf}}\left(1+\frac{1}{\gamma}\right)\frac{\partial^2 u}{\partial y^2}+g\beta_T(T-T_\infty)+g\beta_C(C-C_\infty)-\frac{\sigma_{nf}B_0^2u}{\rho_{nf}}$$

$$=\frac{\mu_{nf}}{\rho_{nf}}\left(1+\frac{1}{\gamma}\right)\left(\frac{a^2x}{\nu_{bf}}\right)f'''+g\beta(T_w-T_\infty)\theta+g\beta^*(C_w-C_\infty)\Phi-\frac{\sigma B_0^2(axf')}{\rho}$$

$$=a^2x\left(\frac{\mu_{nf}}{\rho_{nf}\nu_{bf}}\left(1+\frac{1}{\gamma}\right)f'''+\frac{g\beta(T_w-T_\infty)\theta}{a^2x}+\frac{g\beta^*(C_w-C_\infty)\Phi}{a^2x}-\frac{\sigma B_0^2}{a\rho}f'\right).$$

Hence,

$$a^2x(f'f'-ff'')=a^2x\left(\frac{\mu_{nf}}{\rho_{nf}\nu_{bf}}\left(1+\frac{1}{\gamma}\right)f'''+\frac{g\beta(T_w-T_\infty)\theta}{a^2x}+\frac{g\beta^*(C_w-C_\infty)\Phi}{a^2x}-\frac{\sigma B_0^2}{a\rho}f'\right)$$

$$\frac{\mu_{nf}}{\rho_{nf}\nu_{bf}}\left(1+\frac{1}{\gamma}\right)f'''-(f')^2+ff''+\frac{g\beta(T_w-T_\infty)\theta}{a^2x}+\frac{g\beta^*(C_w-C_\infty)\Phi}{a^2x}-\frac{\sigma B_0^2}{a\rho}f'=0.$$

Setting the parameters

$$Gr_t = \frac{g\beta(T_w - T_\infty)}{a^2 x};\ \ Gr_s = \frac{g\beta^*(C_w - C_\infty)}{a^2 x};\ M = \frac{\sigma B_0^2}{a\rho}\ ;$$

the non-dimensional momentum equation becomes

$$\frac{\mu_{nf}}{\rho_{nf}\nu_{bf}}\left(1 + \frac{1}{\gamma}\right)f''' - f'f' + ff'' + Gr_t\theta + Gr_s\Phi - Mf' = 0.$$

Next is the energy equation

$$u\frac{\partial T}{\partial x} + v\frac{\partial T}{\partial y} = 0 - \left((av)^{\frac{1}{2}}f\right)\left(\left(\frac{a}{\nu}\right)^{\frac{1}{2}}(T_w - T_\infty)\theta'\right) = -(T_w - T_\infty)af\theta'$$

$$\alpha_{nf}\frac{\partial^2 T}{\partial y^2} + \tau\left(\frac{D_B}{\Delta C}\frac{\partial C}{\partial y}\frac{\partial T}{\partial y} + \frac{D_T}{T_\infty}\left(\frac{\partial T}{\partial y}\right)^2\right) + \frac{\mu_{nf}}{(\rho c_P)_{nf}}\left(\frac{\partial u}{\partial y}\right)^2 + \frac{\sigma_{nf}B_0^2 u^2}{(\rho c_p)_{nf}}$$

$$= \alpha_{nf}\left(\frac{a(T_w - T_\infty)}{\nu_{bf}}\right)\theta'' + \frac{\tau a D_B}{\nu\Delta C}(C_w - C_\infty)(T_w - T_\infty)\Phi'\theta'$$

$$+ \frac{\tau a D_T}{\nu_{bf}T_\infty}(T_w - T_\infty)^2(\theta')^2 + \frac{\mu_{nf}}{(\rho c_P)_{nf}}\left(axf''\sqrt{\frac{a}{\nu_{bf}}}\right)^2 + \frac{\sigma_{nf}B_0^2 a^3 x^2}{a(\rho c_p)_{nf}}(f')^2$$

And equating the left-hand side and the right-hand side;

$$-(T_w - T_\infty)af\theta' = \alpha_{nf}\left(\frac{a(T_w - T_\infty)}{\nu_{bf}}\right)\theta'' + \frac{\tau a D_B}{\nu_{bf}\Delta C}(C_w - C_\infty)(T_w - T_\infty)\Phi'\theta'$$

$$+ \frac{\tau a D_T}{\nu_{bf}T_\infty}(T_w - T_\infty)^2(\theta')^2 + \frac{\mu_{nf}}{(\rho c_P)_{nf}}\left(axf''\sqrt{\frac{a}{\nu_{bf}}}\right)^2 + \frac{\sigma_{nf}B_0^2 a^3 x^2}{a(\rho c_p)_{nf}}(f')^2$$

and by rearranging,

$$\alpha_{nf}\left(\frac{a(T_w-T_\infty)}{\nu_{bf}}\right)\theta'' + (T_w-T_\infty)af\theta' + \frac{\tau a D_B}{\nu_{bf}}(T_w-T_\infty)\Phi'\theta' + \frac{\tau a D_T}{\nu_{bf}T_\infty}(T_w-T_\infty)^2(\theta')^2$$

$$+\frac{\mu_{nf}a^3x^2}{(\rho c_P)_{nf}\nu_{bf}}(f'')^2 + \frac{\sigma_{nf}B_0^2a^2x^2}{(\rho c_p)_{nf}}(f')^2 = 0$$

Dividing through by $a(T_w-T_\infty)$, we have

$$\left(\frac{\alpha_{nf}}{\nu_{bf}}\right)\theta'' + f\theta' + \frac{\tau D_B}{\nu_{bf}}\Phi'\theta' + \frac{\tau D_T(T_w-T_\infty)}{\nu_{bf}T_\infty}(\theta')^2 + \frac{\mu_{nf}a^2x^2(f'')^2}{(\rho c_P)_{nf}(T_w-T_\infty)\nu_{bf}}$$

$$+\frac{\sigma_{nf}B_0^2ax^2(f')^2}{(T_w-T_\infty)(\rho c_p)_{nf}} = 0$$

Now, we know that

$$\alpha_{nf} = \frac{k_{nf}}{(\rho c_P)_{nf}} = \frac{\left(\frac{k_{np}+2k_{bf}-2\phi(k_{bf}-k_{np})}{k_{np}+2k_{bf}+\phi(k_{bf}-k_{np})}\right)k_{bf}}{(1-\phi)(\rho c_P)_{bf}+\phi(\rho c_P)_{np}}$$

By setting

$$A_1 = \frac{\left(\frac{k_{np}+2k_{bf}-2\phi(k_{bf}-k_{np})}{k_{np}+2k_{bf}+\phi(k_{bf}-k_{np})}\right)}{\left((1-\phi)+\phi\frac{(\rho c_P)_{np}}{(\rho c_P)_{bf}}\right)};\ \alpha_{bf} = \frac{k_{bf}}{(\rho c_P)_{bf}};$$

Then $\alpha_{nf} = A_1\alpha_{bf}$ and thus,

$$\left(\frac{A_1\alpha_{bf}}{\nu_{bf}}\right)\theta'' + f\theta' + \frac{\tau D_B}{\nu_{bf}}\Phi'\theta' + \frac{\tau D_T(T_w-T_\infty)}{\nu_{bf}T_\infty}(\theta')^2$$

$$+\frac{\mu_{nf}a^2x^2(f'')^2}{(\rho c_P)_{nf}(T_w-T_\infty)\nu_{bf}} + \frac{\sigma_{nf}B_0^2ax^2(f')^2}{(T_w-T_\infty)(\rho c_p)_{nf}} = 0$$

so that

$$A_1\theta'' + \frac{\nu_{bf}}{\alpha_{bf}} f\theta' + \frac{\tau D_B}{\alpha_{bf}}\Phi'\theta' + \frac{\tau D_T (T_w - T_\infty)}{\alpha_{bf} T_\infty}(\theta')^2 + \frac{\mu_{nf} a^2 x^2 (f'')^2}{(\rho c_P)_{nf}(T_w - T_\infty)\alpha_{bf}} + \frac{\nu_{bf}\sigma_{nf} B_0^2 a x^2 (f')^2}{\alpha_{bf}(T_w - T_\infty)\left(\rho c_p\right)_{nf}} = 0$$

Setting the parameters as

$$Pr = \frac{\nu_{bf}}{\alpha_{bf}};\ N_b = \frac{\tau D_B}{\alpha_{bf}};\ N_t = \frac{\tau D_T (T_w - T_\infty)}{\alpha_{bf} T_\infty};\ Ec = \frac{a^2 x^2}{(C_P)_{nf}(T_w - T_\infty)};\ M = \frac{\sigma_{nf} B_0^2}{a\rho_{nf}};$$

the non-dimensional energy equation becomes

$$A_1\theta'' + Prf\theta' + N_b\Phi'\theta' + N_t(\theta')^2 + \frac{\mu_{nf}}{\rho_{nf}\nu_{bf}} Pr\, Ec(f'')^2 + PrMEc(f')^2 = 0.$$

Finally, we non-dimensionalise the concentration equation

$$u\frac{\partial C}{\partial x} + v\frac{\partial C}{\partial y} = D_B\frac{\partial^2 C}{\partial y^2} + \frac{D_T \Delta C}{T_\infty}\frac{\partial^2 T}{\partial y^2}.$$

We proceed as follows

$$0 - \left(a\nu_{bf}\right)^{\frac{1}{2}} f\left(\left(\frac{a}{\nu_{bf}}\right)^{\frac{1}{2}}(C_w - C_\infty)\Phi'\right) = D_B\left(\frac{a}{\nu_{bf}}\right)(C_w - C_\infty)\Phi'' + \frac{D_T\Delta C}{T_\infty}\left(\frac{a}{\nu_{bf}}\right)(T_w - T_\infty)\theta'',$$

$$\Rightarrow \frac{aD_B(C_w - C_\infty)}{\nu_{bf}}\Phi'' + a(C_w - C_\infty)\Phi' f + \frac{D_T\Delta C}{T_\infty}\left(\frac{a}{\nu_{bf}}\right)(T_w - T_\infty)\theta'' = 0,$$

$$\Rightarrow \Phi'' + \frac{\nu_{bf}}{D_B}\Phi' f + \frac{D_T}{D_B T_\infty}(T_w - T_\infty)\theta'' = 0.$$

Setting the parameter $Sc = \frac{\nu}{D_B}$ then

$$\Phi'' + Sc\Phi' f + \frac{N_t}{N_b}\theta'' = 0.$$

Next is to non-dimensionalise the initial and boundary conditions

$$u = ax, \qquad v = 0, \qquad -k_f \frac{\partial T}{\partial y} = h_f\big(T_f - T\big), \qquad C = C_w, \qquad \text{at } \; y = 0$$

$$u = 0, \qquad T = T_\infty, \qquad C = C_\infty, \qquad \text{as } \; y \to \infty.$$

Clearly, at $y = 0$, we have $\eta = 0$ and $\eta \to \infty$ as $y \to \infty$. Thus;

$$u = ax \Rightarrow f'(0) = 1; \;\; v = 0 \Rightarrow f(0) = 0;$$

$$-k_f \frac{\partial T}{\partial y} = h_f\big(T_f - T\big) \Rightarrow -k_f \left(\frac{a}{\nu}\right)^{\frac{1}{2}} (T_w - T_\infty)\theta' = h_f(T_w - T_\infty - (T_w - T_\infty)\theta);$$

$$\theta' = -\frac{h_f}{k_f}\sqrt{\frac{\nu}{a}}(1 - \theta) \Rightarrow \theta'(0) = -Bi(1 - \theta); \;\; \text{where } Bi = \frac{h_f}{k_f}\sqrt{\frac{\nu}{a}}$$

$$C = C_w \Rightarrow \phi(0) = 0;$$

$$u \to 0 \Rightarrow f' \to 0; T \to T_\infty \Rightarrow \theta \to 0; C \to C_\infty \Rightarrow \phi \to 0; \quad \text{as } \eta \to \infty$$

Finally, we have the dimensionless equations as

$$\frac{\mu_{nf}}{\rho_{nf}\nu_{bf}}\left(1 + \frac{1}{\gamma}\right) f''' - f'f' + ff'' + Gr_t\theta + Gr_s\Phi - Mf' = 0,$$

$$A_1\theta'' + Prf\theta' + N_b\Phi'\theta' + N_t(\theta')^2 + \frac{\mu_{nf}}{\rho_{nf}\nu_{bf}} PrEc(f'')^2 + PrMEc(f')^2 = 0,$$

$$\Phi'' + Sc\Phi' f + \frac{N_t}{N_b}\theta'' = 0.$$

with the initial and boundary conditions

$$\text{at } \eta = 0; \qquad f(0) = 0; f'(0) = 1; \theta'(0) = -Bi(1-\theta);\ \phi(0) = 0;$$

$$as\ \eta \to \infty; \qquad f' \to 0, \qquad \theta \to 0;\ \phi \to 0.$$

Gr_t and Gr_s is the thermal and solutal Grashof parameter, M is the magnetic parameter, Pr is the Prandtl number, N_b and N_t are the Brownian and thermophoretic parameter, Ec is the Eckert number and Sc is Schmidt number.

To rewrite these equations as a system of first order ordinary differential equations, set

$$X_1 = f, \qquad X_2 = f', \qquad X_3 = f'', \qquad X_4 = \theta, \qquad X_5 = \theta', \qquad X_6 = \Phi, \qquad X_7 = \Phi$$

So that the equations becomes

$$X_1' = X_2, \tag{4.5}$$

$$X_2' = X_3 \tag{4.6}$$

$$X_3' = \left(\frac{\mu_{nf}}{\rho_{nf}\nu_{bf}}\left(1 + \frac{1}{\gamma}\right)\right)^{-1} (X_2^2 - X_1X_3 - Gr_tX_4 - Gr_sX_6 + MX_2) \tag{4.7}$$

$$X_4' = X_5 \tag{4.8}$$

$$X_5' = \frac{1}{A_1}\left(-PrX_1X_5 - N_bX_5X_7 - N_tX_5^2 + \frac{\mu_{nf}}{\rho_{nf}\nu_{bf}}PrEc{X_3}^2 + PrMEcX_2^2\right) \tag{4.9}$$

$$X_6' = X_7 \tag{4.10}$$

$$X_7' = -ScX_1X_7 - \frac{N_t}{N_b}X_6'. \tag{4.11}$$

with the initial and boundary conditions

$$X_1(0) = 0, \quad X_2(0) = 1, \quad X_5(0) = -Bi\big(1 - X_4(0)\big), \quad X_6(0) = 0 \tag{4.12}$$

$$X_2(\infty) \to 0, \quad X_4(\infty) \to 0, \; X_6(\infty) \to 0. \tag{4.13}$$

The boundary conditions are converted to initial conditions

$$X_1(0) = 0, \;\; X_2(0) = 1, \;\; X_3(0) = s_1, \;\; X_4(0) = 0, \;\; X_5(0) = s_2, \;\; X_6(0) = 0, \;\; X_7(0) = s_3 \tag{4.14}$$

and s_1, s_2 and s_3 are obtained using Shooting Technique to ensure that

$$X_5(0) = -Bi\big(1 - X_4(0)\big), \quad X_2(\infty) \to 0, \quad \text{and} \quad X_4(\infty) \to 1$$

are satisfied.

4.2 Numerical Method

The resulting system of ODEs are solved numerically using the Runge-Kutta-Gills method. The Runge-Kutta scheme of the fourth order for the first order ordinary differential equation

$$y' = f(x, y)$$

is given as

$$y_{n+1} = y_n + \frac{1}{6}(K_1 + 2K_2 + 2K_3 + K_4)$$

$$K_1 = hf(x_n, y_n),\ K_2 = hf\left(x_n + \frac{h}{2}, y_n + \frac{1}{2}K_1\right),$$

$$K_3 = hf\left(x_n + \frac{h}{2}, y_n + \frac{1}{2}K_2\right),\ K_4 = hf(x_n + h, y_n + K_3).$$

The Runge-Kutta-Gills scheme is a modification of the Runge-Kutta scheme which is stable for $h \leq \frac{2.8}{\lambda}$ and it is given as

$$y_{n+1} = y_n + \frac{1}{6}(K_1 + 2bK_2 + 2dK_3 + K_4)$$

$$K_1 = hf(x_n, y_n),\ K_2 = hf\left(x_n + \frac{h}{2}, y_n + \frac{1}{2}K_1\right),$$

$$K_3 = hf\left(x_n + \frac{h}{2}, y_n + aK_1 + bK_2\right),\ K_4 = hf(x_n + h, y_n + cK_2 + dK_3),$$

with constants chosen as

$$a = \frac{\sqrt{2}-1}{2},\ b = \frac{2-\sqrt{2}}{2},\ c = \frac{\sqrt{2}}{2},\ d = \frac{2+\sqrt{2}}{2}.$$

Chapter 5
Discussion of Results

The flow of electrically conducting nanofluid made from Engine oil as base fluid and Copper Cu nanoparticle over a convectively heated vertical surface is studied herewith. See table (1) for the thermophysical properties of the base fluid and the nanoparticles. Unless otherwise stated, the values of the parameters used are $\gamma = 1;\ Gr_t = 1;\ Gr_s = 3;\ M = 3;\ Pr = 7.62;\ Ec = 0.1; \phi = 0.01;\ N_t = 0.1;\ N_b = 0.1;\ Sc = 0.62;\ Bi = 0.1.$

Material	$\boldsymbol{\rho\ (kg/m^3)}$	$\boldsymbol{c_p(J/kgK)}$	$\boldsymbol{k(W/mk)}$	$\boldsymbol{\beta(K^{-1})}$	$\boldsymbol{\sigma(S/m)}$
Engine oil	804	1909	0.145	70×10^{-5}	1.00×10^{-7}
Copper (Cu)	8933	385	401	1.67×10^{-5}	5.96×10^{7}

Table 1: *Thermophysical properties of Engine oil and nanoparticles*

The magnetic field applied normal to the direction of fluid flow induces the Lorentz force which inhibits fluid motion. This is revealed in Figure (2) where the primary velocity reduces with increasing magnetic field strength. The internal friction generated from the reduced velocity produces more heat energy and thereby increases the temperature of the flow as shown in figure (3). Biot number is the ratio of internal resistance to conduction to the resistance of flow to convective heat transfer. As the resistance to conductive heat transfer increases, flow temperature increases and this is as seen in figure (4). The flow tends to a Newtonian flow as Casson parameter γ increases and flow properties are inhibited. Hence, the flow temperature and flow velocity reduces as $\gamma \to \infty$ and this is depicted in figures (5) and (6). Increase in Eckert number leads to an increase the flow velocity and flow temperature (see figures (7) and (8)). Meanwhile increase in

the nanoparticle volume fraction leads to quick sedimentation of the nanoparticles at the wall surface, thereby inhibiting fluid flow and heat transfer. This is evident in figures (9) and (10) where the flow velocity and flow temperature decreases as ϕ increases.

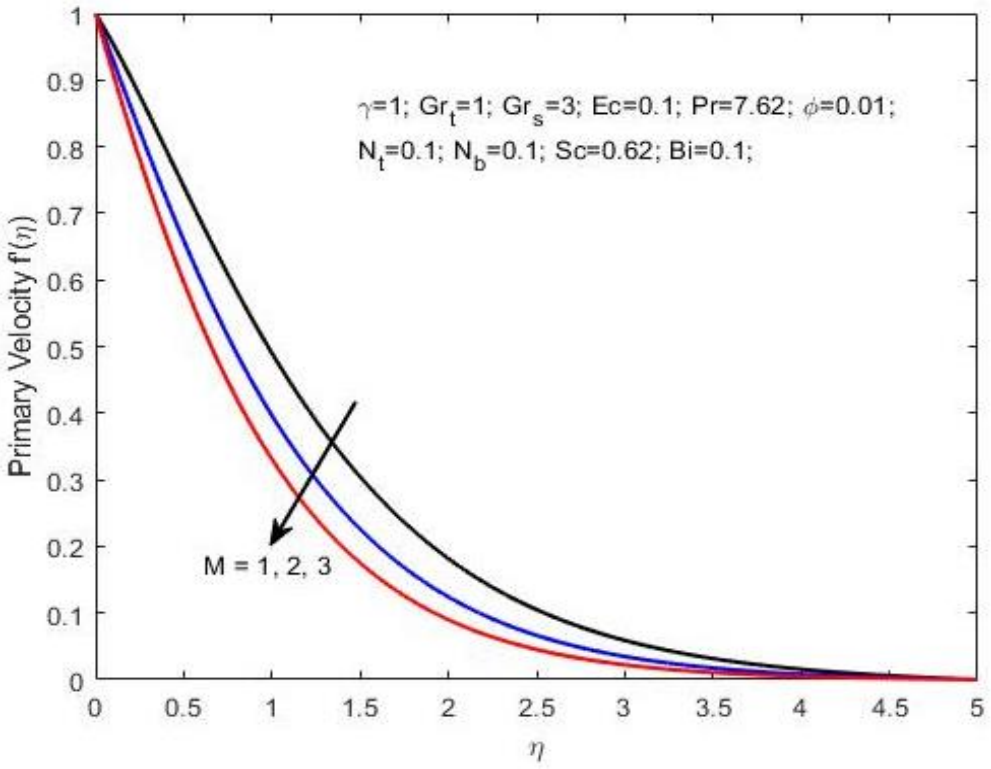

Figure 2: *Variation of primary velocity with magnetic field strength*

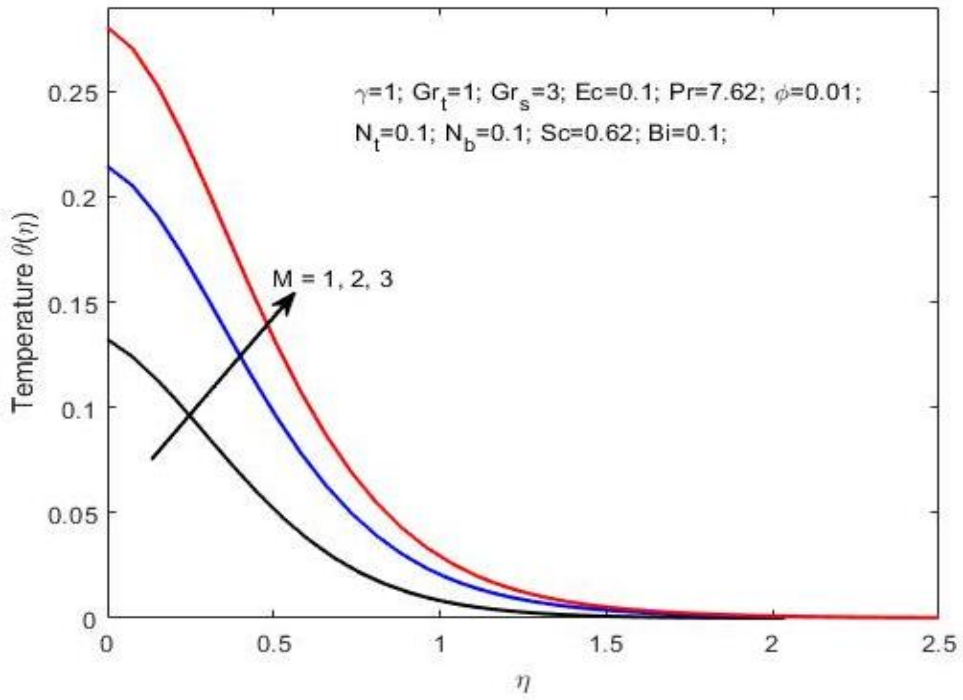

Figure 3: *Variation of temperature with magnetic field strength*

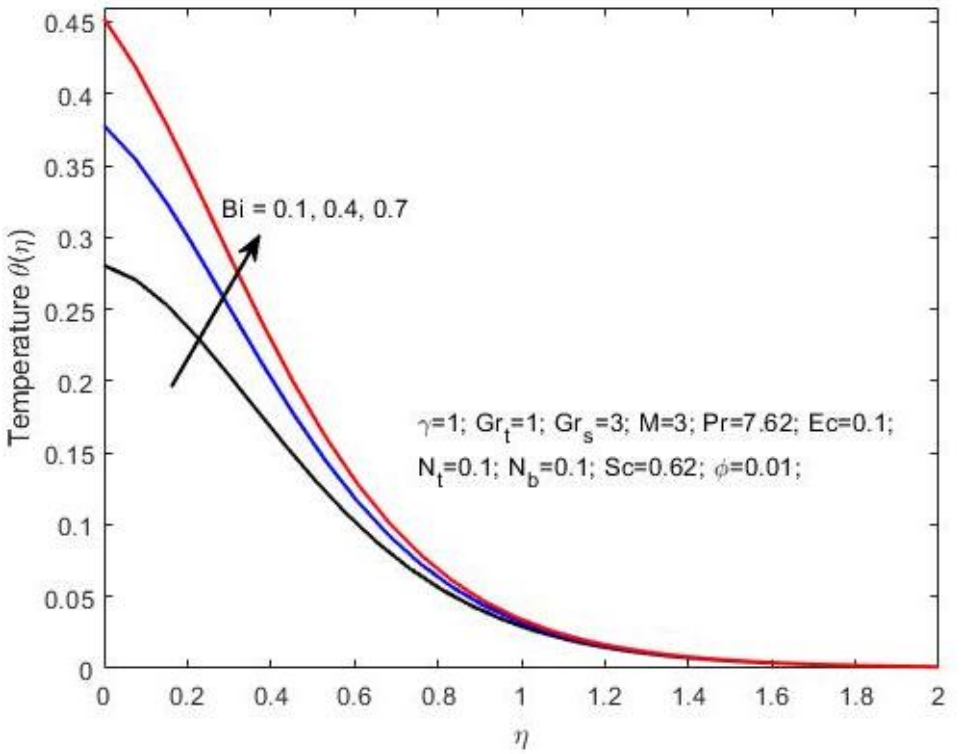

Figure 4: *Variation of temperature with Biot number*

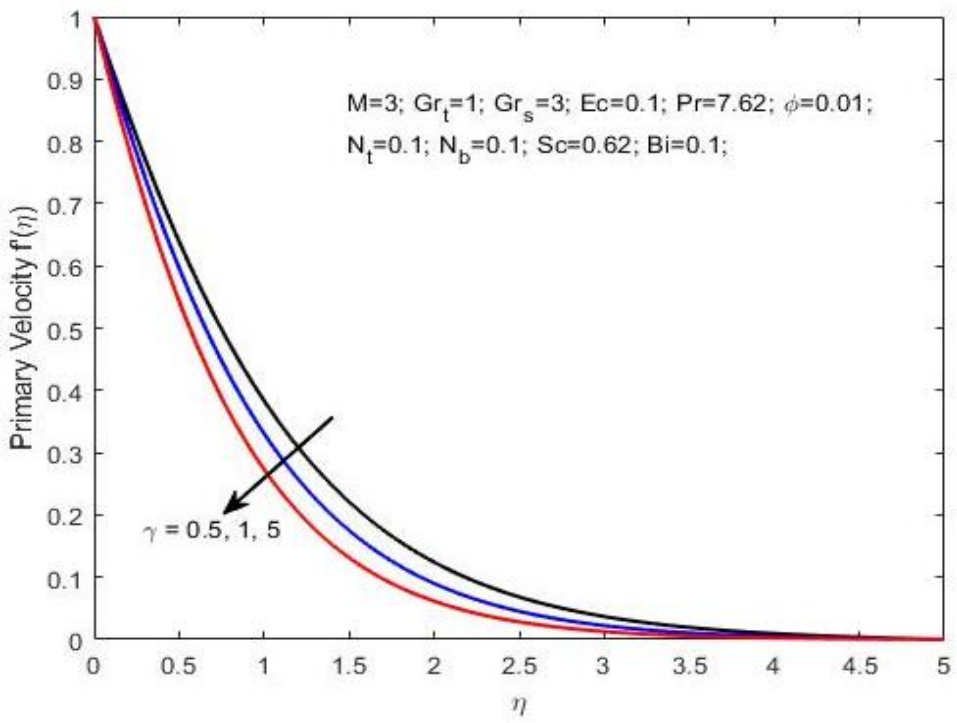

Figure 5: *Variation of primary velocity with Casson fluid parameter*

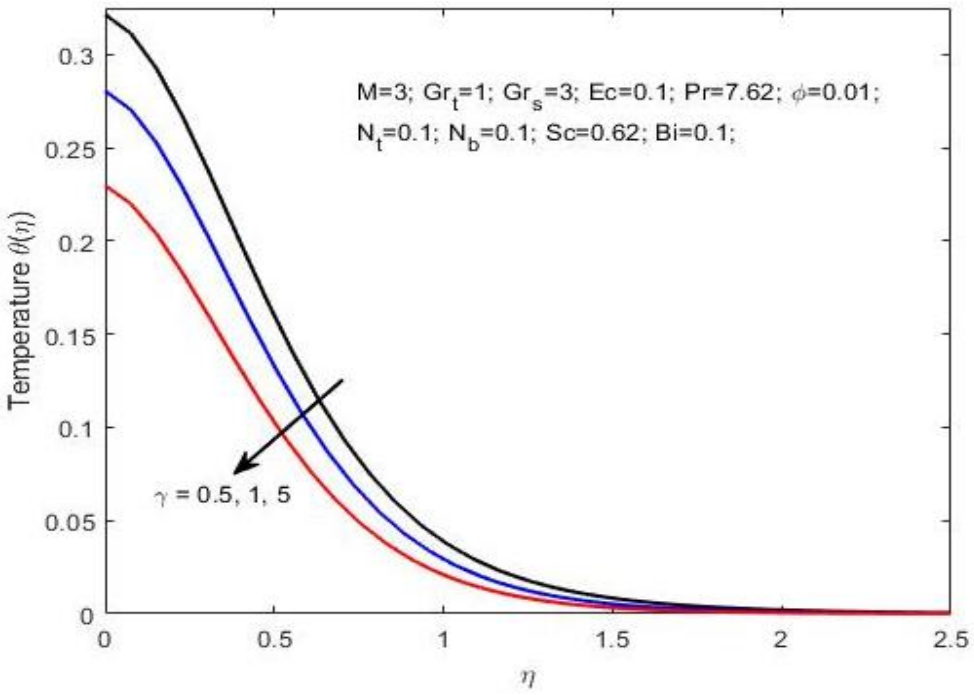

Figure 6: *Variation of temperature with Casson fluid parameter*

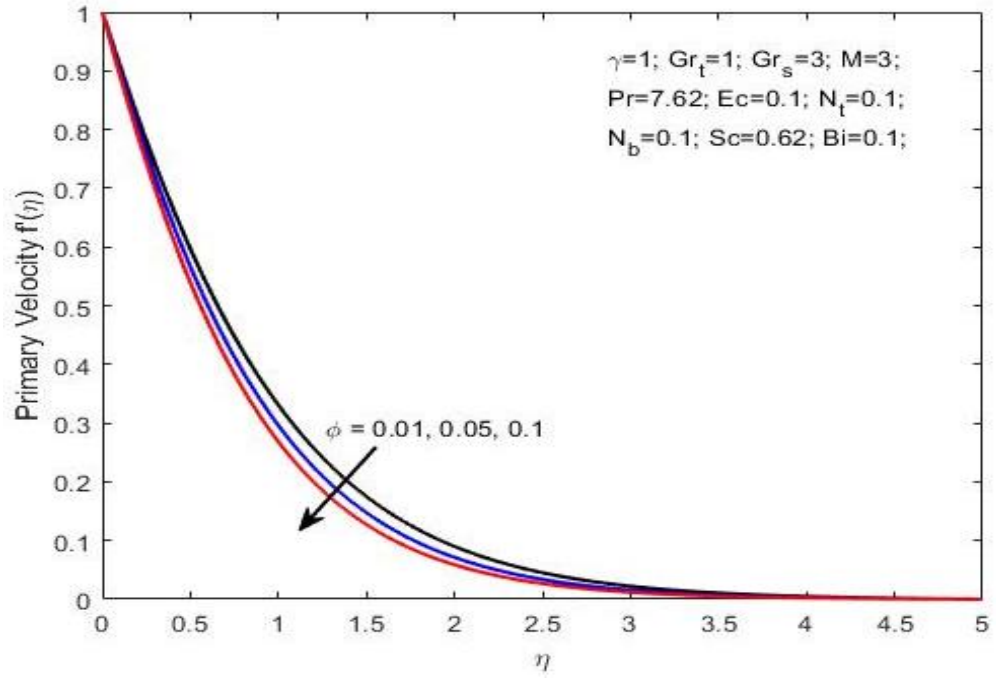

Figure 7: *Variation of primary velocity with nanoparticle volume fraction*

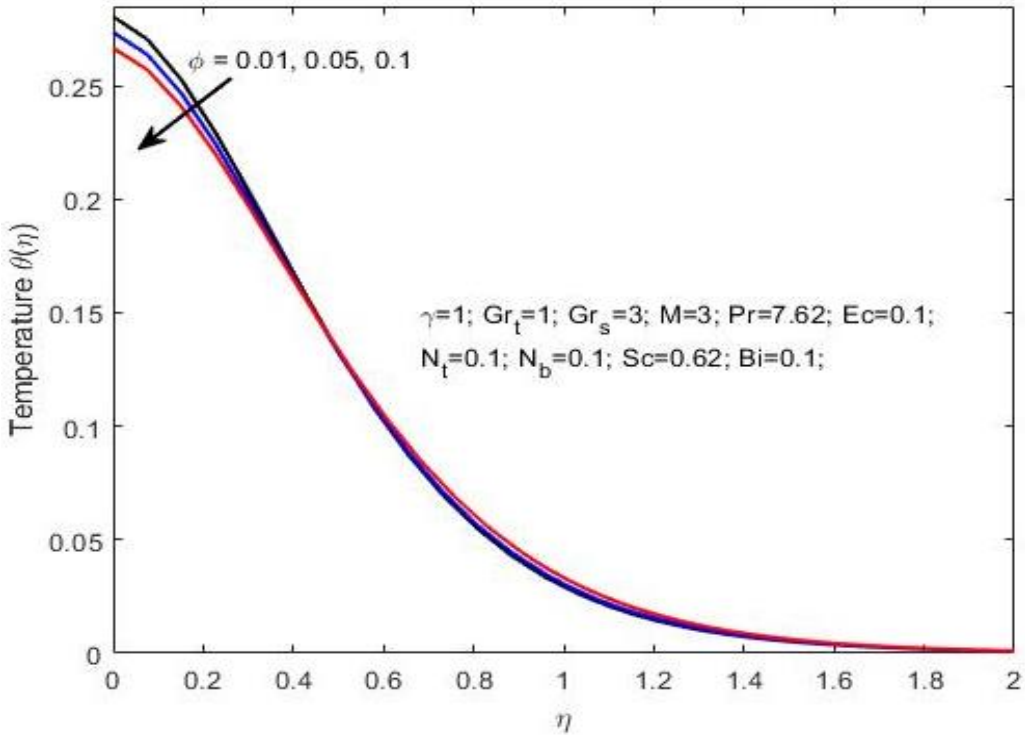

Figure 8: *Variation of temperature with nanoparticle volume fraction*

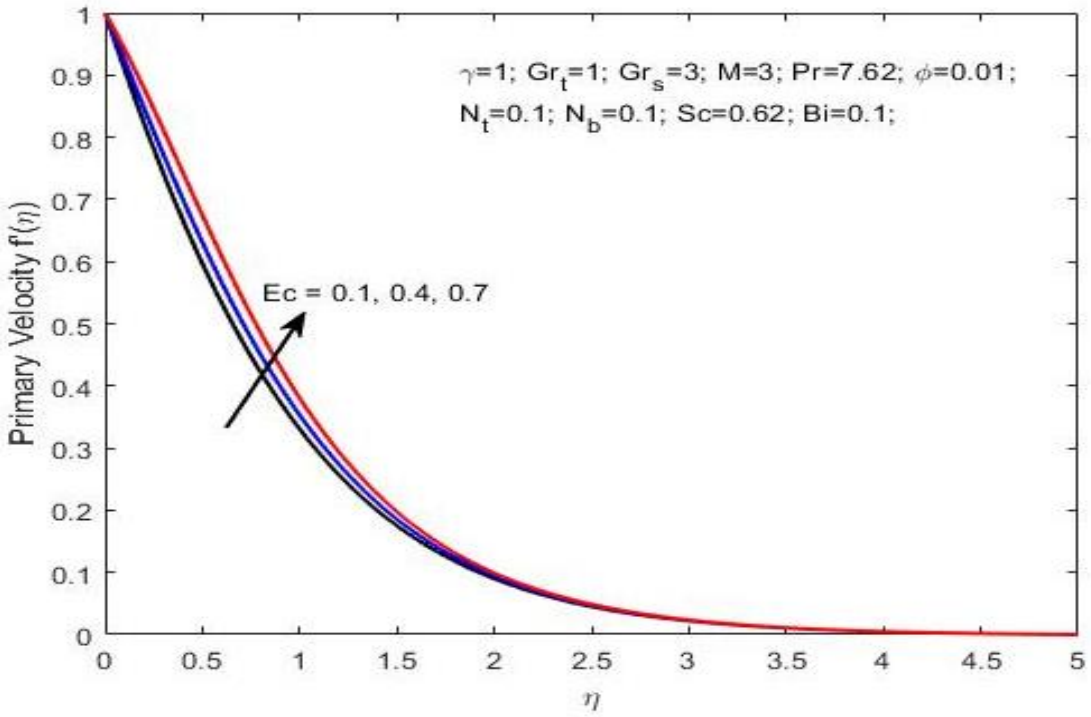

Figure 9: *Variation of primary velocity with Eckert number*

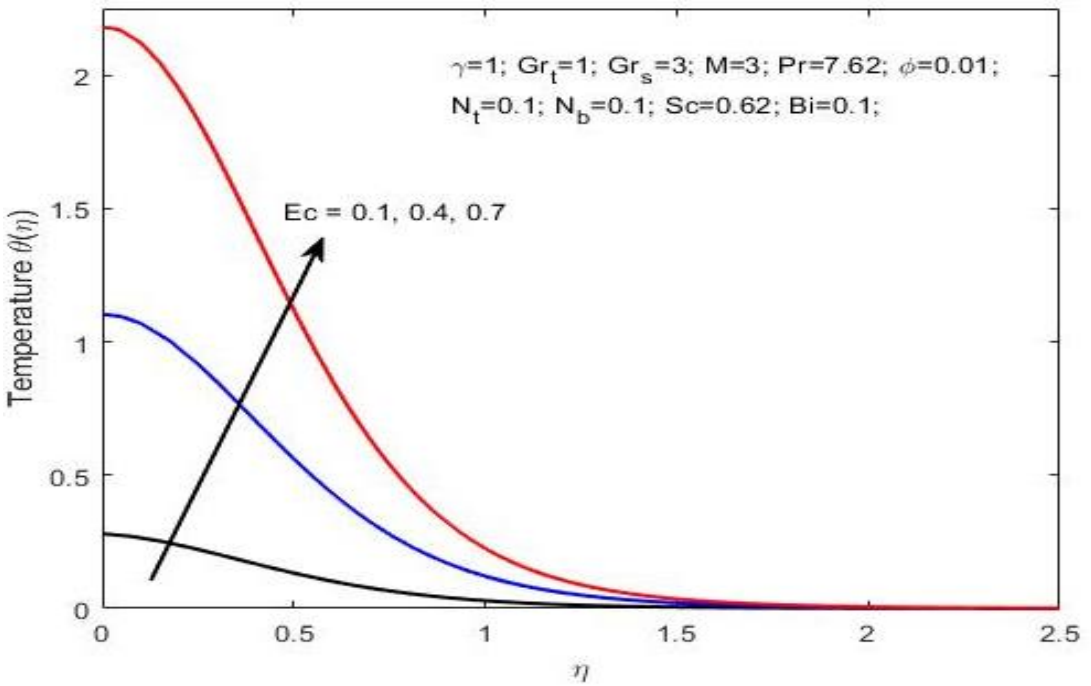

Figure 10: *Variation of temperature with Eckert number*

Chapter 6
Conclusion and Recommendation

A natural convective heat transfer in magnetohydrodynamic flow of Cu-Casson nanofluid over a convectively heated stretching vertical surface is analysed in this project. The equations governing the flow is formulated. The similarity variables are used to nondimensionalised the governing equations and the resulting system of ordinary differential equations is solved using Runge-Kutta-Gills method. Results are depicted in graphs and the following are observed;

1. The primary velocity reduces with increasing magnetic field strength.
2. Flow temperature increases with increasing Biot number.
3. The flow temperature and flow velocity decrease as the Casson fluid parameter increases.
4. Increase in Eckert number leads to an increase the flow velocity and flow temperature.
5. Increase in the nanoparticle volume fraction reduces flow velocity and flow temperature.

Having considered the heat and mass transfer in the flow of Cu-Casson nanofluid over a vertical stretching sheet in the presence of magnetic force in this project, the following recommendations are proposed;

1. The unsteady form of the flow is of practical importance in industrial processes; hence it is recommended that further research can be carried out to study the unsteady form.
2. For a more practical purpose, the flow can be considered in a three-dimensional case.

References

Ahmad, I., Sajid, M., Awan, W., Rafique, M., Aziz, W., Ahmed, M., Abbasi, A., and Taj, M. (2014). MHD flow of a viscous fluid over an exponentially stretching sheet in a porous medium. Journal of Applied Mathematics, 2014:256761.

Ahmad, S., Yousaf, M., Khan, A., and Zaman, G. (2018). Magnetohydrodynamic fluid flow and heat transfer over a shrinking sheet under the influence of thermal slip. Heliyon, 4(30364604):e00828–e00828.

Bulinda, V. M., Kangethe, G. P., and Kiogora, P. R. (2020). Magnetohydrodynamics free convection flow of incompressible fluids over corrugated vibrating bottom surface with hall currents and heat and mass transfers. Journal of Applied Mathematics, 2020:2589760.

Chen, W. Z., Yang, Q. S., Dai, M. Q., and Cheng, S. M. (1998). An analytical solution of the heat transfer process during contact melting of phase change material inside a horizontal elliptical tube. International Journal of Energy Research, 22(2):131–140.

Dincer, I. and Dost, S. (1996). A simple model for heat and mass transfer in absorption cooling systems (acss). International Journal of Energy Research, 20(3):237–243.

Farooq, U., Lu, D., Munir, S., Ramzan, M., Suleman, M., and Hussain, S. (2019). MHD flow of Maxwell fluid with nanomaterials due to an exponentially stretching surface. Scientific Reports, 9(1):7312.

Gbadeyan, J. A., Titiloye, E. O., and Adeosun, A. T. (2020). Effect of variable thermal conductivity and viscosity on casson nanofluid flow with convective heating and velocity slip. Heliyon, 6:e03076.

Idowu, A. S., Akolade, M. T., Abubakar, J. U., and Falodun, B. O. (2020). Mhd free convective heat and mass transfer flow of dissipative casson fluid with variable viscosity and thermal conductivity effects. Journal of Taibah University for Science.

Jabeen, K., Mushtaq, M., and Akram, R. M. (2020). Analysis of the MHD boundary layer flow over a nonlinear stretching sheet in a porous medium using semi-analytical approaches. Mathematical Problems in Engineering, 2020:3012854.

Kataria, H. R. and Patel, H. R. (2018). Heat and mass transfer in magnetohydrodynamic (MHD) Casson fluid flow past over an oscillating vertical plate embedded in porous medium with ramped wall temperature. Propulsion and Power Research, 7(3):257 – 267.

Kolenko, T., Glogovac, B., and Jaklic, T. (1999). An analysis of a heat transfer model for situations involving gas and surface radiative heat transfer. Communications in Numerical Methods in Engineering, 15(5):349–365.

Kumar, B. V. R., Murthy, P. V. S. N., and Singh, P. (1998). Free convection heat transfer from an isothermal wavy surface in a porous enclosure. Int. J. Numer. Meth. Fluids, 28:633–661.

Mahantesh, N. M., Kemparaju, M. C., and Raveendra, N. (2020). Double-diffusive free convective flow of casson fluid due to a moving vertical plate with non-linear thermal radiation. World Journal of Engineering, 14(1):851–862.

Maiga, S. E. B., Nguyen, C. T., Galanis, N., and Roy, G. (2004). Heat transfer behaviours of nanofluids in a uniformly heated tube. Superlattices Microstructures, 35:543–557.

Mustafa, M. and Khan, J. A. (2015). Model for flow of Casson nanofluid past a non-linearly stretching sheet considering magnetic field effects. AIP Advances, 5(077148).

Mutuku, W. N. (2016). Ethylene glycol (EG)-based nanofluids as a coolant for automotive radiator. Asia Pac. J. Comput. Engin. 3(1).

Mutuku-Njane, W. N. and Makinde, O. D. (2013). Combined effect of buoyancy force and Navier slip on MHD flow of a nanofluid over a convectively heated vertical porous plate. The Scientific World Journal Volume, Article ID 725643, 2013.

Nadeem, S., Haq, R. U., Akbar, N. S., and Khan, Z. H. (2013). MHD three-dimensional Casson fluid flow past a porous linearly stretching sheet. Alexandria Engineering Journal, 52(4):577–582.

Pak, B. C. and Cho, Y. I. (1998). Hydrodynamic and heat transfer study of dispersed fluids with submicron metallic oxide particles. Experimental Heat Transfer: A Journal of Thermal Energy Generation, Transport, Storage, and Conversion, 11(2):151–170.

Piechowski, M. (1998). Heat and mass transfer model of a ground heat exchanger: validation and sensitivity analysis. International Journal of Energy Research, 22(11):965–979.

Pramanik, S. (2014). Casson fluid flow and heat transfer past an exponentially porous stretching surface in presence of thermal radiation. Ain Shams Engineering Journal, 5(1):205 – 212.

Saatdjian, E., Lam, R., and Mota, J. P. B. (1999). Natural convection heat transfer in the annular region between porous confocal ellipses. International Journal for Numerical Methods in Fluids, 31(2):513–522.

Shah, Z., Kumam, P., and Deebani, W. (2020). Radiative mhd casson nanofluid flow with activation energy and chemical reaction over past nonlinearly stretching surface through entropy generation. Scientific Reports, 10(1):4402.

Venkateswarlu, S., K., V. S. V., and Durga, P. P. (2020). MHD flow of MoS_2 and MgO water based nanofluid through porous medium over a stretching surface with cattaneo-christov heat flux model and convective boundary condition. International Journal of Ambient Energy, 0(0):1–10.

Wasp, F. J. (1977). Solid-liquid flow slurry pipeline transportation. Trans. Tech. Pub., Berlin.

Xuan, Y. and Roetzel, W. (2000). Conceptions for heat transfer correlation of nanofluids. International Journal of Heat and Mass Transfer, 43(19):3701–3707.

Yang, Y.-T., Chen, C.-K., and Chi-Fang (1996). Convective heat transfer from a circular cylinder under the effect of a solid plane wall. International Journal for Numerical Methods in Fluids, 23(2):163–176.

Zerroukat, M., Power, H., and Chen, C. S. (1998). A numerical method for heat transfer problems using collocation and radial basis functions. International Journal for Numerical Methods in Engineering, 42(7):1263–1278.

Appendices

MATLAB Codes

The boundary condition

```
function res = Bc(y0,yinf)
    global gamma Grt Grs M Pr Ec cp_np cp_bf k_bf k_np
   global phi rho_np rho_bf Nt Nb Sc Bi
    res = [y0(1);
          y0(2)-1;
          y0(5)-Bi*(y0(4)-1);
          y0(6)-1;
          yinf(2);
          yinf(4);
          yinf(6)];
end
```

The system of ordinary differential equations

```
function res = Fluid(eta,x)
    global gamma Grt Grs M Pr Ec cp_np cp_bf k_bf k_np
   global phi rho_np rho_bf Nt Nb Sc Bi
   rho_cp_np = rho_np*cp_np;
   rho_cp_bf = rho_bf*cp_bf;

    A1     =     (k_np     +     2*k_bf-2*phi*(k_bf-k_np))     /
((k_np+2*k_bf+phi*(k_bf-k_np))    *(1-phi    +    phi*rho_cp_np
/rho_cp_bf));
    A2 = 0.904*exp(0.148*phi)/(1-phi+phi*rho_np/rho_bf);

    dx1 = x(2);   dx2 = x(3);
    dx3           =           -(1/(A2*(1+1/gamma)))*(x(1)*x(3)-
x(2)^2+Grt*x(4)+Grs*x(6)-M*x(2));
    dx4 = x(5);
```

```
    dx5  =  -(1/A1)*(Pr*x(1)*x(5)+  Nb*x(7)*x(5)+  Nt*(x(5)^2)  +
Ec*M*Pr*x(2)^2) + A2*Ec*Pr*x(3)^2;
    dx6 = x(7);
   dx7 = -Sc*x(7)-(Nt/Nb)*dx6;
    res = [dx1;dx2;dx3;dx4;dx5;dx6;dx7];
end
```

The bvp4c code

```
clc
global gamma Grt Grs M Pr Ec cp_np cp_bf k_bf k_np
global phi rho_np rho_bf Nt Nb Sc Bi
gamma=1; Grt=1; Grs=3; M=3; Pr=7.62; Ec=0.1;
phi=0.01; Nt=0.1; Nb=0.1; Sc=0.62; Bi=0.1;
rho_bf=804; cp_bf=1909; k_bf=0.145;         %base fluid
rho_np=8933; cp_np=385;   k_np=401;         %Cu
Values=[0.5,1,5];
for i=1:3
    gamma=Values(i);
    solinit=bvpinit(linspace(0,5,100),[0 0 0 0 0 0 0]);
    sol= bvp4c(@Fluid,@Bc,solinit);
    sol.y;
    if i==1
        figure(2), plot(sol.x,sol.y(2,:),'k-','LineWidth',1)
        xlabel('\eta')
        ylabel("Primary Velocity f'(\eta)")
        hold on

        figure(4), plot(sol.x,sol.y(4,:),'k-','LineWidth',1)
        xlabel('\eta')
        ylabel("Temperature \theta(\eta)")
        hold on
    elseif i==2
        figure(2), plot(sol.x,sol.y(2,:),'b-','LineWidth',1)
        xlabel('\eta')
        ylabel("Primary Velocity f'(\eta)")
        hold on

        figure(4), plot(sol.x,sol.y(4,:),'b-','LineWidth',1)
        xlabel('\eta')
```

```
        ylabel("Temperature \theta(\eta)")
        hold on
    elseif i==3
        figure(2), plot(sol.x,sol.y(2,:),'r-','LineWidth',1)
        xlabel('\eta')
        ylabel("Primary Velocity f'(\eta)")
        hold on

        figure(4), plot(sol.x,sol.y(4,:),'r-','LineWidth',1)
        xlabel('\eta')
        ylabel("Temperature \theta(\eta)")
        hold on
    end
end
```